ACS Sustainable Chemistry & Engineering

Research Article

pubs.acs.org/journal/ascecg

Efficient Phosphate Sequestration in Waters by the Unique Hierarchical 3D *Artemia* Egg Shell Supported Nano-$Mg(OH)_2$ Composite and Sequenced Potential Application in Slow Release Fertilizer

Sufeng Wang,[†] Mengxuan Ma,[†] Qingrui Zhang,*[,†] Guiqing Sun,[§] Tifeng Jiao,*[,†] and Robert K. Okazaki[‡]

[†]Hebei Key Laboratory of Applied Chemistry, School of Environmental and Chemical Engineering, Yanshan University, 438 Hebei Avenue, Qinhuangdao 066004, Peoples' Republic of China

[‡]Department of Zoology, Weber State University, 1415 Edvalson Street, Department 2505, Ogden, Utah 84408-2505, United States

[§]Hebei Ocean & Fisheries Science Research Institute, Qinhuangdao 066200, Peoples' Republic of China

Supporting Information

ABSTRACT: *Artemia* nauplii are important bait or food sources in aquaculture, but the egg shells after incubation are always subjected to discarding as natural wastes; therefore, application and utilization of the *Artemia* egg-shell wastes will be an important issue. Herein, we reported a new hybrid biomaterial by encapsulating nano-$Mg(OH)_2$ onto discarded *Artemia* egg shells for phosphate sequestration enhancement. The unique hierarchically 3D-layered structure of *Artemia* egg shells can endow well-defined nano-$Mg(OH)_2$ morphology and efficient phosphate adsorption performances. The results of the final hybrid biomaterial exhibit a wide pH dependent sorption process, strong affinity toward phosphate removal, and large sorption capacity. Moreover, the exhausted adsorbent shell−Mg-P can be further utilized as slow-release fertilizer without regular chemical regeneration. The efficient slow-release behaviors of phosphorus onto Shell−Mg−P for 30 days indicated the potential applicability as fertilizers. Additionally, the actual seedling tests further confirm that the shell−Mg−P can be readily used as a slow-release fertilizer for the soil improvement and crop productivity.

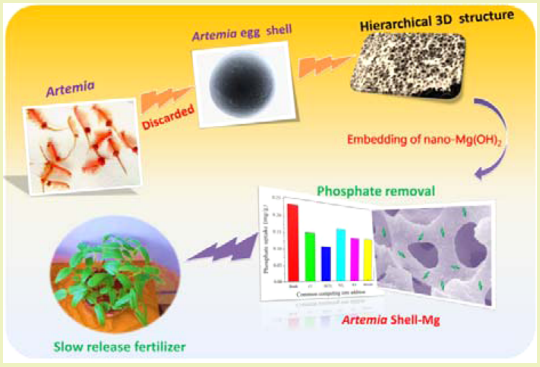

KEYWORDS: *Biomaterial, Artemia egg shell, Waste, Plant grown*

INTRODUCTION

Large quantities of phosphorus, coming from excessive emission of agricultural or industruial point source pollution, can lead to serious eutrophication and profuse algal growth in natural waters even at trace levels,[1,2] This anthropogenic effect will contribute negatively on the environment and human health. Thus, finding an effective approach to balance the increasing phosphate input into waters becomes an urgent goal. As yet, various efficient methods have been proposed, including chemical precipitation,[3] biological treatment,[4,5] membrane extraction[6,7] and adsorption process,[8−10] to address the potential phosphate sequestration. Aiming at the enhanced trace phosphates removal, adsorption technology might be a favorable choice due to its efficient performances and economical views.

Recently, nanosized alkaline earth metal oxides, which are nontoxic and environmentally friendly, have become increasingly important in environmental applications. One such metal oxide, $Mg(OH)_2$, is commonly used in various adsorption usages because of its large surface areas/active sites, the simple large-scale production from abundant natural minerals[11] and highly selective sorption performances.[12−15] For instance, the micro-/nanostructure-$Mg(OH)_2$, prepared by a bulk $MgCO_3$ calcination process, exhibits significant dye wastewater enrichment of ∼4000-fold[14] and efficient recyclable phosphate properties in seawater.[16] Our recent study also demonstrated the preferential phosphate adsorption with strong capability onto $Mg(OH)_2$ nanocomposites.[11] Such efficient performances can be attributed to the following characteristics: (1) the high zero potential (12.4) providing sufficient $Mg(OH)_2$ positive surfaces charges, which always exhibits much wider sorption pH ranges, suitable for adsorption of anion pollutants, e.g. phosphate ions;[17,18] (2) the potential formation of strong inner-sphere complexation between Mg−OH and the target phosphates, which has been demonstrated in our previous study;[11,19] and (3) the nanoscale morphology can further provide available activated sites toward phosphate removal. However, similar to the conventional inorganic adsorbents,

Received: June 28, 2015
Revised: August 30, 2015
Published: September 13, 2015

DOI: 10.1021/acssuschemeng.5b00594
ACS Sustainable Chem. Eng. 2015, 3, 2496−2503

magnesium oxide/hydroxide currently cannot be used directly in fixed bed or any other flow-through systems, because of the technical difficulties in solid−liquid separation and large hydraulic resistances.[20,21]

To overcome previously mentioned problems, an alternative route is to prepare the hybrid materials by immobilizing nano-$Mg(OH)_2$ particles onto various porous matrices with large grain sizes, e.g., activated carbon,[19,22,23] chitosan,[24] or macroporous polymers.[25,26] Such a hybridized strategy will readily attain the separation purposes. Meanwhile, the porous nanostructure of carriers can further immobilize the embedded nano-$Mg(OH)_2$, which potentially can be an important step forward engineering nanoparticles for phosphate sequestration. Nevertheless, the efficient hybrid sorbents are still suffering from serious hurdles, e.g., (1) the consumption of high concentration alkaline solution for regeneration, (2) the low sorption-regeneration stability due to Mg(II) releases, and (3) the disposal of high phosphate concentrations in regenerated effluent, which requires further chemical precipitation by $Ca(OH)_2$ or $CaCl_2$, resulting in large amounts of sludge accumulation. These difficulties are major obstacles in developing efficient hybrid sorbents especially from the standpoint of commercial applicability. Besides, the highly concentrated phosphates onto hybrid $Mg(OH)_2$ materials cannot be further utilized as the recycling resources. Phosphate is an important nutrient, if the exhausted phosphate-loaded hybrid materials can then be used as a sequenced slow release fertilizer to achieve resource exploitation,[27−29] which will be a significant development for sustainable functional materials application. Thus, an ideal carrier material is needed with the following three conditions: (1) the skeleton of carriers should be biocompatible, even biodegradable for fertilizer demands in soil; (2) the unique pore channels of the matrix should ensure a slow phosphate release process under varying soil chemical conditions and microorganism surroundings; (3) the used supporter will be low-cost and an eco-friendly material, exhibiting low utilization and/or creation of wastes.

Artemia nauplii are important bait or food sources in aquaculture. They are usually distributed in most of the salt fields or lakes,[30−32] located in mainly developed and developing nations, e.g., the United States, India, China, Japan, Europe Union, etc. According to statistics, a total of 180 000 tons of *Artemia* per year will be hatched for cultivation demands.[33] The discarded egg shells are always disposed as wastes after nauplii collection. Moreover, *Artemi*a egg shell exhibits excellent biocompatibility and environmentally friendly properties with mainly the components of chitosan or chitin, calcium, and ferric compounds.[34,35] Different from the traditional biomaterials, *Artemia* egg shell shows distinguished chemical stability, due to its environmental exposures of high salts, radiation, low temperatures, and extreme anoxic conditions. More importantly, the *Artemi*a egg shell also displays a unique heterogeneous 3D pore structure morphology with abundant micropore matrix and microporous arrangements.[36,37] These properties will (1) enhance the embedded $Mg(OH)_2$ for its immobilization and (2) provide fast kinetic diffusion toward phosphate sequestration and slow-release behavior for fertilizer application.

Our present research will report on the fabrication of a new hybrid biomaterial (denoted *Artemia* shell−Mg) by impregnating nano-$Mg(OH)_2$ onto the heterogeneous 3D structural *Artemia* egg shell. This transformed *Artemia* shell−Mg will be shown to increase the retention of phosphate and how the sequenced exhausted phosphate-loaded adsorbents can be recycled and utilized as a slow-release fertilizer in soils. The phosphate uptake behaviors onto *Artemia* shell−Mg and the subsequent phosphate release characteristics as fertilizers along with the corresponding seedling growth will also be described.

MATERIALS AND METHODS

Materials. All the reagents (Tianjin Reagent Station Co) were analytical grade. The stocks of phosphate were prepared by dissolving KH_2PO_4 salts in deionized water as the phosphorus sources. The *Artemia* egg shells were collected as a host matrix from the Beidaihe Central Experiment Station of the Chinese Academy of Fishery Science. Prior to use, the obtained shells were subjected to washing with the deionized water to remove the residual impurities (including salts) and then vacuum desiccated at 60 °C to a constant weight. The soil used in the study was collected from the campus of Yanshan University, and the mung beans were selected as the seeding samples.

Preparation of the Hybrid *Artemia* Shell-Mg Material. The synthesis of target hybrid biomaterial was carried out by precursor diffusion and an *in situ* precipitation process. Briefly, 5 g of treated *Artemia* shells was immersed into 100 mL of a magnesium nitrate solution (1 M) at room temperature under 4 h of ultrasound (100 Hz, 25 °C) and subsequently agitated mechanically for 20 h. The fast adsorption process occurs between *Artemia* egg shells (mainly composing of ammonium groups-NH_2 of chitosan) and precursor Mg(II) with obtaining the intermediate products *Artemia* shell/Mg^{2+}. Next, the resulting *Artemia* shell/Mg^{2+} was filtrated and then immersed into 400 mL of NaOH solution (1% mass fraction) for 16 h. Finally, the products were desiccated at 60 °C in a vacuum oven for nano-$Mg(OH)_2$ immobilization, resulting in the successful yield of hybrid *Artemia* shell−Mg. Final *Artemia* shell−Mg composites were completely washed in distilled water to achieve neutral pH's, prior to experimental uses.

Phosphate Sorption Behaviors onto *Artemia* Shell-Mg. The phosphate uptake was carried out by the conventional bottle-point methods. The detailed experimental procedures were presented as follows: the solution pH effects on phosphate adsorption were determined by adding 0.4 g of *Artemia* shell−Mg sorbents into 50 mL solutions containing certain contents of phosphates at desired temperatures. The above mixtures were then transferred into an incubator shaker (SHA-85, China) and shaken under 200 rpm for 20 h at desired temperatures to ensure the sorption equilibrium. Solution pH can be adjusted by using dilute HNO_3 and NaOH solutions. To evaluate the potential applicability of *Artemia* shell−Mg for phosphate sequestration, the common ubiquitous ions, including Cl^-, NO_3^-, HCO_3^-, and humic acid (HA), were used to estimate the sorption selectivity. Similar to the conventional batch tests, 0.4 g of *Artemia* shell−Mg was added into 50 mL of 2.5 mg/L phosphate solutions with different levels of competing ions present. After the vessels were shaken completely to ensure the sorption equilibrium, the final phosphate concentrations at equilibrium were then determined.

Adsorption kinetics of phosphate on *Artemia* shell−Mg were determined by mixing 0.4 g of adsorbents with 1000 mL phosphate solutions (30 mg/L) in flasks at room temperature (25 ± 0.5 °C). The vessels were then shaken in a mechanical shaker. Kinetics data were calculated by measuring the sample contents at various intervals.

Slow Phosphate Release Behavior from *Artemia* Shell-Mg. The bioavailability of phosphorus and slow release experiments were performed by using the conventional Mehlich3 method with an extracting volumetric ratio of 1:10.[38,39] The Mehlich3 extractants are mainly composed of 0.2 M CH_3COOH, 0.25 M NH_4NO_3, 0.015 M NH_4F, 0.013 M HNO_3, and 0.001 M EDTA with final pH values of approximately 2.5 ± 0.1. The mixtures of the exhausted *Artemia* shell−Mg and Mehlich3 extractant were shaken at 200 rpm for 5 min at room temperature (25 ± 0.5 °C), and then the released phosphorus concentrations were determined.

A total of 1 g of exhausted *Artemia* shell−Mg (denoted as shell−Mg−P) was introduced into 1000 mL of distilled water, and the released phosphate concentrations at various time intervals were

DOI: 10.1021/acssuschemeng.5b00594
ACS Sustainable Chem. Eng. 2015, 3, 2496−2503

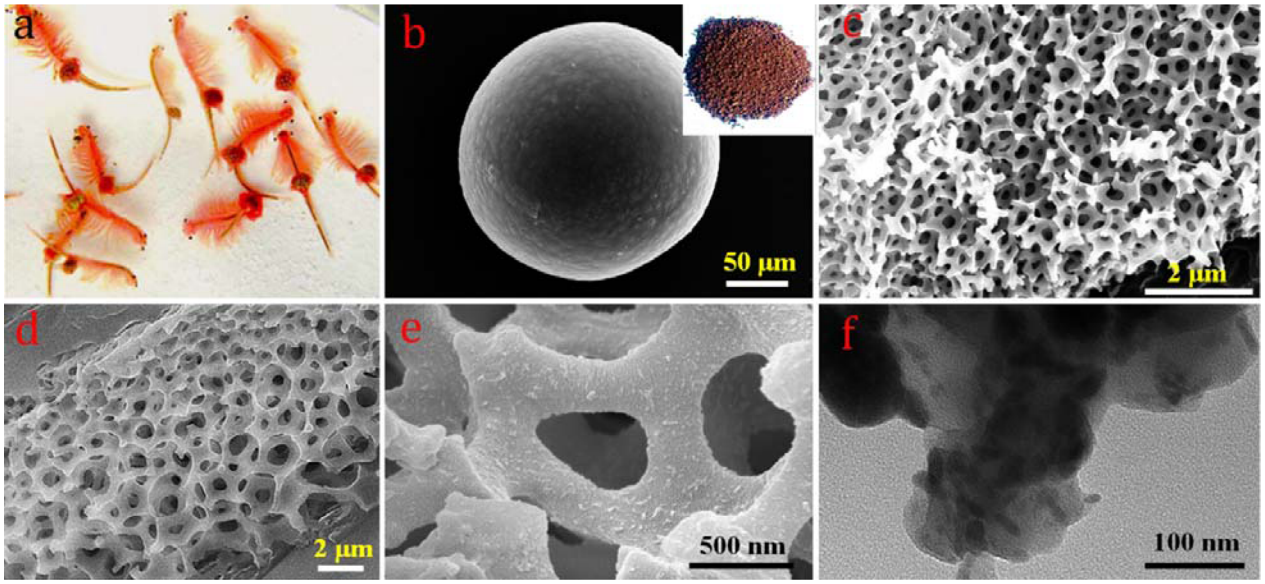

Figure 1. Microscopy characterization of the hybrid biomaterials. (a) Live *Artemia*; (b) SEM image of *Artemia* egg shell; (c) SEM of pore structures of the *Artemia* shell; (d) SEM of pore structures of *Artemia* shell−Mg; (e) higher magnification of SEM *Artemia* shell−Mg; (f) TEM analysis of resulting *Artemia* shell−Mg.

determined. It is noteworthy that the fresh distilled water will be displaced after 24 h release tests. Additionally, the phosphorus release behaviors at different pHs were also concerned according to the similar procedures.

To further investigate the slow-release performance under soil conditions, 1 g of the resulting shell−Mg−P was buried in a container with 50 g of dry soil (<18 meshes, 880 μm), and then spraying water was conducted until saturation. The standard substance KH_2PO_4 was also involved for a reference based on the equal phosphate amounts.

After 24 h of incubation, 10 mL of water was sprinkled evenly on the sample and produced a leachate; the concentration of phosphate in the leachate was tested. The leaching process was repeated at intervals of 24 h. The experimental data were collected during 30 day tests.

Seed Germination and Early Stage Seedling Growth Bioassay. The seed germination and early stage seedling growth bioassay experiments were performed by spreading the same number of seeds on the surface layer of soils at identical environment surroundings. Both the primitive *Artemia* shell−Mg and shell−Mg−P were involved for fertility contrast, and all replicates were incubated in an illumination incubator and set on a 12-h light/12-h dark photoperiod. Seeds germinated successfully were counted and observed. After 15 days of seedling growth, the weight and the height of the leaves were well measured, respectively.

Analytical Methods. The concentration of phosphate was determined by the molybdenum blue spectrophotometric method with a UV−vis spectrophotometer at 700 nm (Hitachi-DR/5000, USA). The surface morphology and element analysis of *Artemia* shell−Mg were performed using field emission scanning electron microscopy (FESEM; S-4800 II, Hitachi, Japan), equipped with an energy dispersive X-ray spectrometer (EDS; Horiba, Japan). TEM images were recorded using a high-resolution transmission electron microscope (HRTEM, JEM2010) to observe the embedded nano-$Mg(OH)_2$ particles onto the porous surface of *Artemia* egg shells. X-ray diffraction (XRD) using an XTRA X-ray diffractometer (Switzerland) is used for identifying the crystalline pattern. Statistical analysis was performed using SPSS 11.0 statistical software with significant differences ($P < 0.05$) among means being tested by one-way ANOVA followed by Duncan's multiple range tests.

RESULTS AND DISCUSSION

Characterization of the Resultant *Artemia* Shell−Mg. The synthesized biomaterial *Artemia* shell−Mg was well characterized by SEM, EDS, TEM, and XRD analysis. The image of live *Artemia* nauplii is presented in Figure 1a, and its discarded egg shell (Figure 1b) after incubation remains spherical in shape with a size approximated at 200−250 μm. Interestingly, its profile (Figure 1c) exhibits a hierarchically 3D-layered structure with a wide pore range (100 nm to 2 μm), which is mainly composited of chitosan or chitin and ferric and calcium substances by EDS analysis (Figure S1). Figure 1d reveals that the $Mg(OH)_2$ particles are successfully embedded into the skeleton surfaces of *Artemia* egg shell, and its corresponding magnifying image further demonstrates that the embedded $Mg(OH)_2$ particles exhibit a rod shape with a size ~40 nm in length and ~10 nm in width (Figure 1e). The nanoscale morphology formation can be attributed to the present strong affinity between the ammonium groups within a chitosan matrix and Mg(II) precursor, which has been demonstrated by SenGupta et al. and in our previous study.[40,41] TEM analysis (Figure 1f) further proves the successful encapsulation of nano-$Mg(OH)_2$ rods, and the sizes coincide with the SEM results. The XRD pattern (Figure 2) suggests that the embedded Mg(II) species exist in the form of low-crystalline magnesium hydroxide. Phosphate uptake was

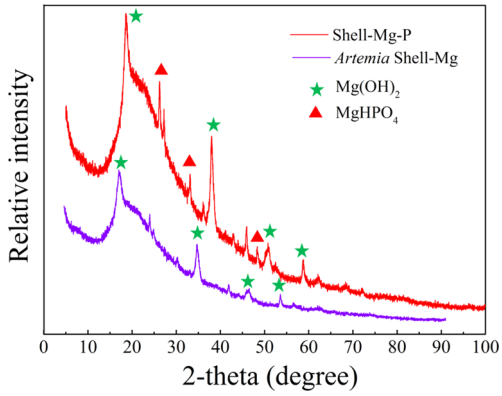

Figure 2. XRD pattern of the *Artemia* shell−Mg and the phosphate loaded *Artemia* shell−Mg.

DOI: 10.1021/acssuschemeng.5b00594
ACS Sustainable Chem. Eng. 2015, 3, 2496−2503

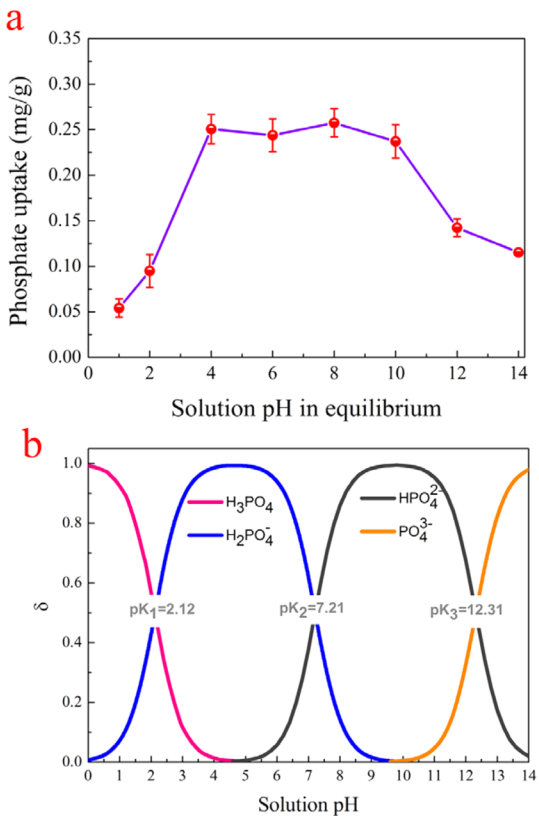

Figure 3. (a) Solution pH effects on phosphate adsorption (conditions: dose 0.4 g, 50 mL solution at 298 K, initial phosphate content of 2.5 mg/L). (b) Phosphate species distributions at various solution pH's.

observed notably to bring about the formation of $MgHPO_4$ particles.

Phosphate Adsorption Behaviors onto *Artemia* Shell−Mg. The effects of pH on phosphate uptake show that phosphate adsorption is a pH-dependent process with the optimal pH ranging from 4.0 to 10.0 (Figure 3a). These results reveal that the *Artemia* shell−Mg exhibits much wider available sorption conditions than other metal oxides. Considering the high zero potentials (9.8−12.4) of $Mg(OH)_2$,[42,43] the present protonated $MgOH_2^+$ will favor a preferential adsorption toward $H_2PO_4^-/HPO_4^{2-}$ species. However, further increasing the solution pH (pH > 11.0) will form the deprotonated MgO^- species, which can exert strong repulsive force toward negatively charged phosphate sequestration. Note that, at extremely alkaline conditions (pH > 14), the irreversible adsorption capacity indicates the possible presence of a coprecipitation mechanism for phosphate removal. Additionally, the adsorption of phosphate tends to decrease gradually between pH 1.0 and 3.0. This observation is possibly attributed to the phosphorus species transformation from $H_2PO_4^-$ to neutral H_3PO4 (Figure 4b) as well as the encapsulated $Mg(OH)_2$ releases under acidic conditions. Considering that the common coexisting ions, including Cl^-, NO_3^-, and HCO_3^- ions and humic acid (HA), are always ubiquitous in phosphate contaminated waters, it is necessary to evaluate the possible sorption influences on competing ions. Common anion additions were observed to bring about resultant sorption decreases, due to the presence of the high levels of anionic substances (Figure 4a). However, the resulting *Artemia* shell−Mg can still display favorable phosphate adsorption with available sorption efficiencies of ∼40%−60%, which can be

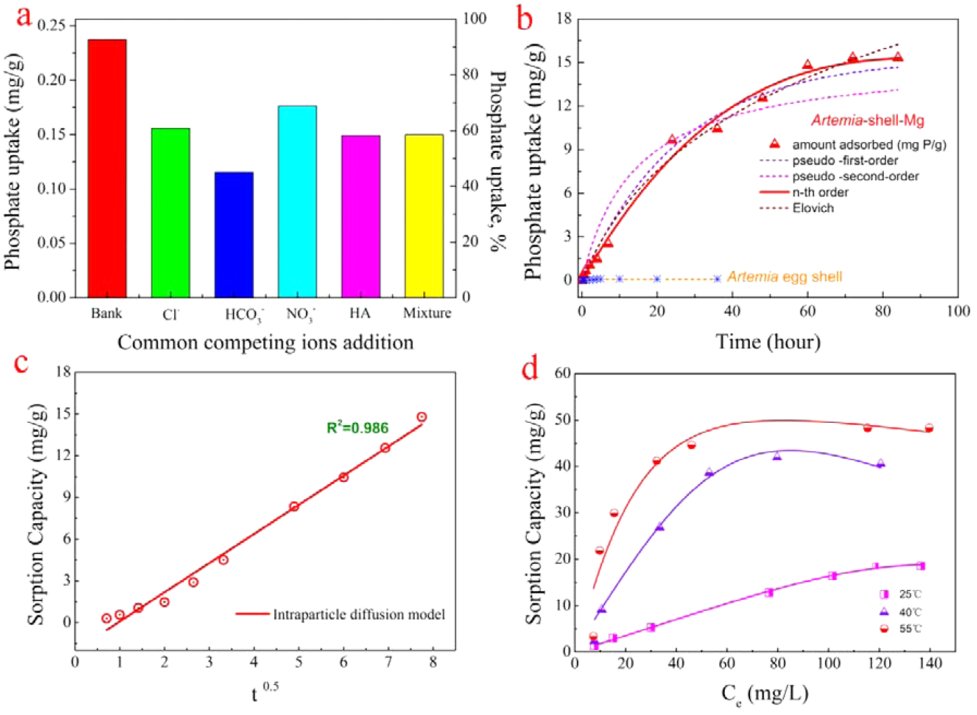

Figure 4. (a) Sorption competition tests toward phosphate removal onto the obtained *Artemia* shell−Mg (conditions: 0.4 g sorbent, 50 mL solution at 298 K, initial phosphate of approximately 2.5 mg/L, Cl^- = 50 mg/L, NO_3^- = 15 mg/L, HCO_3^- = 80 mg/L, and HA = 2 mg/L, pH = 6.4−7.2). (b) Sorption kinetics data and fitting curves. (c) Intraparticle diffusion model for kinetic fitting (kinetic conditions: dose 0.4 g, 1000 mL solution containing 30 mg/L phosphate at 298 K, pH = 6.2−6.8). (d) Adsorption isotherm at different temperatures (conditions: 1g/L, 298 K, pH = 6.4−6.9).

DOI: 10.1021/acssuschemeng.5b00594
ACS Sustainable Chem. Eng. 2015, 3, 2496−2503

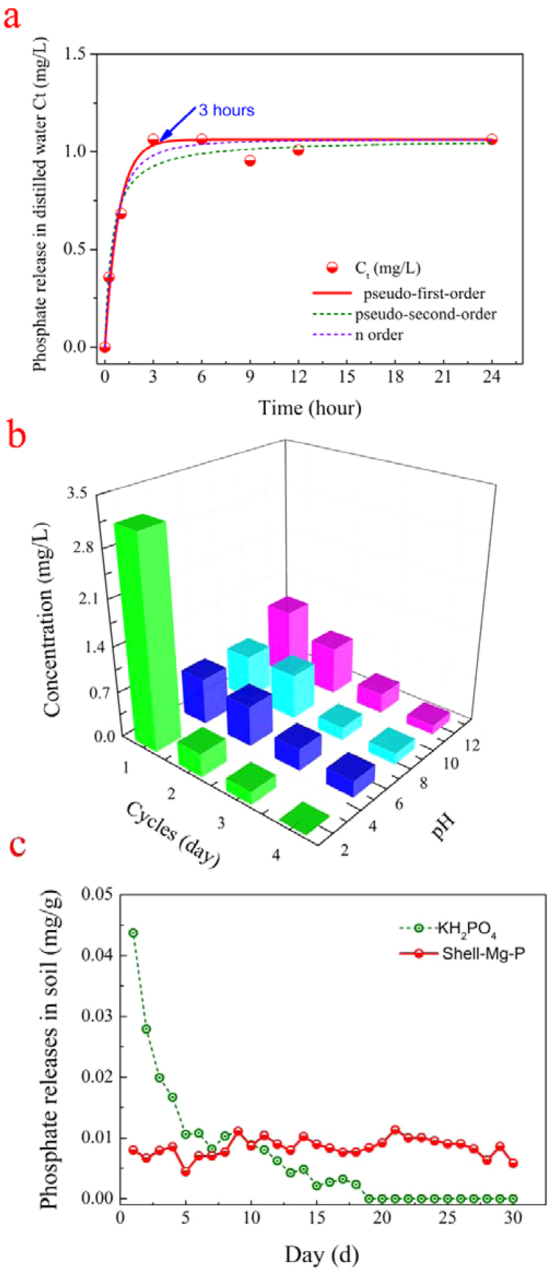

Figure 5. (a) Phosphate release kinetics behavior onto Shell−Mg−P samples in distilled water. (b) pH effect on phosphate release of the resultant Shell−Mg−P. (c) Phosphate slow-release behaviors in actual soil conditions.

attributed to the potential formation of strong inner-sphere complexation through Mg−O−P bonds; this process has been previously demonstrated.[11] Additionally, since this phosphate adsorption has been found to be effective against competitive influences, this process can be utilized subsequently for enhancing the subsequent slow-release fertilizer application.

Sorption kinetic experiments (Figure 4b) suggest that the phosphate uptake is a gradual process. A fast adsorption can be achieved at the beginning 5 h, followed by a slow phosphate uptake for approaching sorption equilibrium within 24 h. This result is similar to the phosphate sorption behaviors onto biochar produced from Mg-enriched tomato tissues and digested sugar beet tailings.[44] Moreover, the classical kinetic models were also conducted to describe the phosphate uptake process.[29]

$$\frac{dq_t}{dt} = k_1(q_e - q_t) \text{ pseudo-first-order} \quad (1)$$

$$\frac{dq_t}{dt} = k_2(q_e - q_t)^2 \text{ pseudo-second-order} \quad (2)$$

$$\frac{dq_t}{dt} = k_n(q_e - q_t)^n \ n\text{th-order} \quad (3)$$

$$\frac{dq_t}{dt} = a \exp(-bq_t) \text{ Elovich} \quad (4)$$

$$q_t = kt^{1/2} \text{ intraparticle diffusion} \quad (5)$$

where q_t (mg/g) and q_e (mg/g) represent the amounts of phosphate uptake at time t and equilibrium, respectively; k_1 (h^{-1}), k_2 ($g{\cdot}mg^{-1}{\cdot}h^{-1}$), and k_n ($g^{n-1}{\cdot}mg^{1-n}{\cdot}h^{-1}$) are the adsorption rate constants, a ($mg{\cdot}g^{-1}{\cdot}h^{-1}$) is the initial adsorption rate, and b ($g{\cdot}mg^{-1}$) denotes the desorption constant. The pseudo-first-order, pseudo-second-order, and nth-order models were used to describe the sorption kinetics in the solid-solution system based on mononuclear, binuclear, and n-nuclear adsorption, respectively, which related to the sorbent capacity. The Elovich model is an empirical equation based on the influences of desorption.

The fitted kinetic parameters of the models are summarized in Table S1. Evidently, the adsorption onto *Artemia* shell−Mg can be well described by the nth-order model as compared to other models, due to the good correlation coefficient (R^2 = 0.993, Table S1), suggesting that phosphate removal can be controlled by multiple mechanisms. The well-fitted Elovich (R^2 = 0.989) and intraparticle diffusion models (R^2 = 0.986, Figure 4c) notably confirm the possible multilayer adsorption mechanism and inner pore diffusion process. Such an interesting kinetic process can be ascribed to the unique heterogeneous 3D structure of the host *Artemia* egg shell. Additionally, the slow kinetic properties for phosphate sorption equilibrium also indicate the possible application as a slow-release fertilizer. It is noteworthy that the primitive *Artemia* eggshell displays negligible adsorption capacity as a reference, due to the lacking of protonated species onto surface ammonium groups.

Moreover, sorption isotherms at different temperatures for phosphate uptake were further investigated (Figure 4d). Phosphate uptake onto *Artemia* shell−Mg is a temperature-dependent endothermic reaction; such results further demonstrate that phosphate removal is dominated by adsorption mechanism rather than the chemical precipitation process. Additionally, to further elucidate the phosphate adsorption process, the classical isotherm models were employed to describe the experimental data with the governing equations as follows:

$$q_e = \frac{k_L Q C_e}{1 + k_L C_e} \text{ Langmuir} \quad (6)$$

$$q_e = k_F C_e^n \text{ Freudlich} \quad (7)$$

$$q_e = \frac{k_R C_e}{1 + a C_e^n} \text{ Redlich−Peterson} \quad (8)$$

DOI: 10.1021/acssuschemeng.5b00594
ACS Sustainable Chem. Eng. 2015, 3, 2496−2503

Figure 6. Effects of control *Artemia* egg shell and shell−Mg−P on mung bean seedling growth.

$$q_e = \frac{RT}{b}\ln(AC_e) \text{ Temkin} \quad (9)$$

where k_L ($L \cdot mg^{-1}$), k_F ($mg^{(1-n)} \cdot L^n \cdot g^{-1}$), and k_R ($L \cdot g^{-1}$) denote the Langmuir bonding term, the Freundlich affinity coefficient, and the Redlich−Peterson isotherm constant, respectively; Q ($mg \cdot g^{-1}$) is assigned to the maximum sorption capacity; C_e ($mg \cdot L^{-1}$) is the phosphate concentration at equilibrium; n is the Freundlich linearity constant; and a ($L^n \cdot mg^{-n}$), b ($J \cdot g \cdot mg^{-1}$), and A ($L \cdot mg^{-1}$) are the Redlich−Peterson isotherm constant and the Temkin isotherm constants, respectively. The detailed parameters were listed in Table S2. It can be detected that the sorption results can be well described by the Redlich−Peterson model with the high R^2 values of 0.999, which suggests the heterogeneous multilayer sorption sites between the embedded nano-$Mg(OH)_2$ and the target phosphate, resulting from the unique porous structure of the matrix *Artemia* egg shell. Additionally, the large sorption capacity (maximum 32.7 mg/g) further proves the efficient phosphate removal as well as sufficient phosphate loadings for the slow-release fertilizer application

Slow-Release Evaluation onto Shell−Mg−P. Considering the specific biocompatibility of *Artemia* egg shells and outstanding phosphate enrichment properties, the exhausted nanocomposites *Artemia* shell−Mg−P could potentially benefit crops and improve Mg(II) and phosphorus supplies in the soils. Therefore, the spent adsorbent may serve as a slow-release phosphate fertilizer for further application. Next, the potential slow-release performances from shell−Mg−P were further evaluated. The biodegradable phosphate contents of the exhausted shell−Mg−P were determined by the conventional Mehlich3 extractable method,[38,39] which is widely used for determining the plant-available phosphorus in soil. The total extractive phosphates from shell−Mg−P is approximately 69.41 ± 2.2 mg P/kg sorbent, which is beyond the nominal capacity as a slow-release fertilizer for optimum P (45−50 mg P/kg) in soil for plant growth and crop yields.[45] This result demonstrates the significant feasibility for fertilizer application.

Furthermore, the slow-release behaviors were then investigated. The phosphate release kinetics in distilled water showed that the phosphate release equilibrium can be approached within 2 h (Figure 5a). Such fast phosphate release might be originated from the phosphate adherence or weak bond reactions. Additionally, the phosphate release behaviors can be well described by the pseudo-first-order model. Additionally, considering the complex acidic and alkaline environment in a soil system, the solution pH effects on the phosphate releases were further explored. As depicted in Figure 5b, a rapid high concentration of phosphate release is observed at low pH conditions (pH < 2), which might be ascribed to the dissolution of the encapsulated $MgHPO_4 \cdot 3H_2O$ particles. Meanwhile, a successively slow-releasing process was detected at weak acidic and neutral or alkaline surroundings for above 4 days, indicating the potential slow release fertilizer application in a wide chemical environment. Moreover, the actual phosphate slow releasing process was further investigated in a real soil environment, and the purified KH_2PO_4 samples were also selected for a reference. The release of phosphorus from the shell−Mg−P and purified KH_2PO_4 in soil is displayed in Figure 5c. After addition into soil, the KH_2PO_4 samples were observed to dissolve and become exhausted quickly while the slow-release response of phosphorus from the shell−Mg−P lasted for 30 days, a strong indication for its potential as a fertilizer for crop growing. The total release amounts for the 30 day period are approximately 65.8% of the phosphate adsorbed.

Effects of Shell−Mg−P As a Fertilizer on Seedling Growth. To further demonstrate the applicability of shell−Mg−P as a slow-release fertilizer, the seedling growth tests were also conducted. The mung bean seedlings were exposed to *Artemia* shell−Mg (controls) and shell−Mg−P (experimental) under identical conditions, and their detailed growth is depicted in Figure 6. After the 15-day experiment, the seeds exposed to the shell−Mg−P showed significant seeding length relative to the control *Artemia* shell-egg. To further confirm the significant differences for seeding growth, statistical analysis was performed using SPSS 11.0 statistical software with significant differences ($P < 0.05$, Table S3) among means being tested by one-way ANOVA followed by Duncan's multiple range tests. The resultant shell−Mg−P exhibits an outstanding seedling length of 12.41 ± 0.85 as compared to the primitive *Artemia* shell (8.50 ± 1.05) and bare soil (7.79 ± 0.94). It further confirms that the shell−Mg−P can be readily used as a slow-release fertilizer for soil improvement and increased crop productivity.

In summary, we reported a new waste utilization by anchoring nano-$Mg(OH)_2$ onto the discarded *Artemia* egg shell. The unique hierarchical 3D pore structure and nano-$Mg(OH)_2$ formation can provide the efficient phosphate removal in waters. The subsequent exhausted adsorbent

DOI: 10.1021/acssuschemeng.5b00594
ACS Sustainable Chem. Eng. 2015, 3, 2496−2503

containing phosphate can then be further used for the slow-release of the fertilizer to minimize labor and costs of its reapplication. This research offers a new approach for the new carrier-nanoparticle adsorbent fabrication and its possible commercial applicability.

■ ASSOCIATED CONTENT

Supporting Information

The Supporting Information is available free of charge on the ACS Publications website at DOI: 10.1021/acssuschemeng.5b00594.

SEM-EDS analysis (Figure S1), XRD spectra of *Artemia* egg shell (Figure S2), Mg(II) release in various solution pH's, the kinetic parameters (Table S1), adsorption isotherm fitting data (Table S2), and the detailed data of seedling lengths (Table S3) (PDF)

■ AUTHOR INFORMATION

Corresponding Authors

*E-mail: zhangqr@ysu.edu.cn. Tel.: +86-335-8387-741. Fax: +86-335-8061-549.

*E-mail: tfjiao@ysu.edu.cn. Tel.: +86-335-8387-741. Fax: +86-335-8061-549.

Notes

The authors declare no competing financial interest.

■ ACKNOWLEDGMENTS

We greatly acknowledge the financial support from the National Natural Science Foundation of China (Grant Nos. 40830746, 41271102, 21207112, 51578476, and 21473153), and the National Science Technology Support Program (Grant No. 2011BAD13B06), as well as the Key Laboratory of Reservoir Aquatic Environment, Chongqing Institute of Green and Intelligent Technology, Chinese Academy of Science (Grant NO. RAE2014CE03B).

■ REFERENCES

(1) Smil, V. Phosphorus in the environment: natural flows and human interferences. *Annu. Rev. Energy Env.* **2000**, *25*, 53−88.

(2) Dodds, W. K. Trophic state, eutrophication and nutrient criteria in streams. *Trends Ecol. Evol.* **2007**, *22*, 669−676.

(3) Huang, H.; Yang, J.; Li, D. Recovery and removal of ammonia−nitrogen and phosphate from swine wastewater by internal recycling of struvite chlorination product. *Bioresour. Technol.* **2014**, *172*, 253−259.

(4) Tu, Y.; Schuler, A. J. Low acetate concentrations favor polyphosphate-accumulating organisms over glycogen-accumulating organisms in enhanced biological phosphorus removal from wastewater. *Environ. Sci. Technol.* **2013**, *47*, 3816−3824.

(5) Santinelli, M.; Eusebi, A.; Santini, M.; Battistoni, P. The zootechnical anaerobic supernatants: nutrient removal by a biological advanced process. *Ind. Eng. Chem. Res.* **2012**, *51*, 5490−5496.

(6) Xie, M.; Nghiem, L. D.; Price, W. E.; Elimelech, M. Toward resource recovery from wastewater: extraction of phosphorus from digested sludge using a hybrid forward osmosis−membrane distillation process. *Environ. Sci. Technol. Lett.* **2014**, *1*, 191−195.

(7) Hasson, D.; Beck, A.; Fingerman, F.; Tachman, C.; Shemer, H.; Semiat, R. Simple model for characterizing a Donnan dialysis process. *Ind. Eng. Chem. Res.* **2014**, *53*, 6094−6102.

(8) Biswas, B. K.; Inoue, K.; Ghimire, K. N.; Harada, H.; Ohto, K.; Kawakita, H. Removal and recovery of phosphorus from water by means of adsorption onto orange waste gel loaded with zirconium. *Bioresour. Technol.* **2008**, *99*, 8685−8690.

(9) Xie, F.; Wu, F.; Liu, G.; Mu, Y.; Feng, C.; Wang, H.; Giesy, J. P. Removal of phosphate from eutrophic lakes through adsorption by in situ formation of magnesium hydroxide from diatomite. *Environ. Sci. Technol.* **2013**, *48*, 582−590.

(10) Rodrigues, L. A.; Maschio, L. J.; Cividanes Coppio, L. d. S.; Thim, G. P.; Caetano Pinto da Silva, M. L. Adsorption of phosphate from aqueous solution by hydrous zirconium oxide. *Environ. Technol.* **2012**, *33*, 1345−1351.

(11) Zhang, Q.; Zhang, Z.; Teng, J.; Huang, H.; Peng, Q.; Jiao, T.; Hou, L.; Li, B. Highly efficient phosphate sequestration in aqueous solutions using nanomagnesium hydroxide modified polystyrene materials. *Ind. Eng. Chem. Res.* **2015**, *54*, 2940−2949.

(12) Chen, Z.; Zhuang, Z.; Cao, Q.; Pan, X.; Guan, X.; Lin, Z. Adsorption-induced crystallization of U-rich nanocrystals on nano-Mg $(OH)_2$ and the aqueous uranyl enrichment. *ACS Appl. Mater. Interfaces* **2014**, *6*, 1301−1305.

(13) Harada, T.; Simeon, F.; Hamad, E. Z.; Hatton, T. A. Alkali metal nitrate-promoted high-capacity MgO adsorbents for regenerable CO_2 capture at moderate temperatures. *Chem. Mater.* **2015**, *27*, 1943−1949.

(14) Wang, Y.; Chen, J.; Lu, L.; Lin, Z. Reversible switch between bulk $MgCO_3 \cdot 3H_2O$ and $Mg(OH)_2$ micro/nanorods induces continuous selective preconcentration of anionic dyes. *ACS Appl. Mater. Interfaces* **2013**, *5*, 7698−7703.

(15) Liu, M.; Xu, J.; Cheng, B.; Ho, W.; Yu, J. Synthesis and adsorption performance of Mg $(OH)_2$ hexagonal nanosheet−graphene oxide composites. *Appl. Surf. Sci.* **2015**, *332*, 121−129.

(16) Loganathan, P.; Vigneswaran, S.; Kandasamy, J.; Bolan, N. S. Removal and recovery of phosphate from water using sorption. *Crit. Rev. Environ. Sci. Technol.* **2014**, *44*, 847−907.

(17) Cao, Q.; Huang, F.; Zhuang, Z.; Lin, Z. A study of the potential application of nano-Mg $(OH)_2$ in adsorbing low concentrations of uranyl tricarbonate from water. *Nanoscale* **2012**, *4*, 2423−2430.

(18) Hunter, R. J. *Zeta Potential in Colloid Science: Principles and Applications*; Academic Press: Waltham, MA, 2013; Vol. 2, pp 894−895.

(19) Zhang, M.; Gao, B.; Yao, Y.; Xue, Y.; Inyang, M. Synthesis of porous MgO-biochar nanocomposites for removal of phosphate and nitrate from aqueous solutions. *Chem. Eng. J.* **2012**, *210*, 26−32.

(20) Pan, B.; Han, F.; Nie, G.; Wu, B.; He, K.; Lu, L. New strategy to enhance phosphate removal from water by hydrous manganese oxide. *Environ. Sci. Technol.* **2014**, *48*, 5101−5107.

(21) Chen, L.; Zhao, X.; Pan, B.; Zhang, W.; Hua, M.; Lv, L.; Zhang, W. Preferable removal of phosphate from water using hydrous zirconium oxide-based nanocomposite of high stability. *J. Hazard. Mater.* **2015**, *284*, 35−42.

(22) Yao, Y.; Gao, B.; Chen, J.; Zhang, M.; Inyang, M.; Li, Y.; Alva, A.; Yang, L. Engineered carbon (biochar) prepared by direct pyrolysis of Mg-accumulated tomato tissues: characterization and phosphate removal potential. *Bioresour. Technol.* **2013**, *138*, 8−13.

(23) Moussavi, G.; Rashidi, R.; Khavanin, A. The efficacy of GAC/MgO composite for destructive adsorption of benzene from waste air stream. *Chem. Eng. J.* **2013**, *228*, 741−747.

(24) Haldorai, Y.; Shim, J.-J. An efficient removal of methyl orange dye from aqueous solution by adsorption onto chitosan/MgO composite: A novel reusable adsorbent. *Appl. Surf. Sci.* **2014**, *292*, 447−453.

(25) Awual, M. R.; Jyo, A.; Ihara, T.; Seko, N.; Tamada, M.; Lim, K. T. Enhanced trace phosphate removal from water by zirconium (IV) loaded fibrous adsorbent. *Water Res.* **2011**, *45*, 4592−4600.

(26) Xu, Z.; Cheng, L.; Shi, J.; Lu, J.; Zhang, W.; Zhao, Y.; Li, F.; Chen, M. Kinetic study of the removal of dimethyl phthalate from an aqueous solution using an anion exchange resin. *Environ. Sci. Pollut. Res.* **2014**, *21*, 6571−6577.

(27) Yetilmezsoy, K.; Sapci-Zengin, Z. Recovery of ammonium nitrogen from the effluent of UASB treating poultry manure wastewater by MAP precipitation as a slow release fertilizer. *J. Hazard. Mater.* **2009**, *166*, 260−269.

(28) Bansiwal, A. K.; Rayalu, S. S.; Labhasetwar, N. K.; Juwarkar, A. A.; Devotta, S. Surfactant-modified zeolite as a slow release fertilizer for phosphorus. *J. Agric. Food Chem.* **2006**, *54*, 4773−4779.

(29) Yao, Y.; Gao, B.; Chen, J.; Yang, L. Engineered biochar reclaiming phosphate from aqueous solutions: mechanisms and potential application as a slow-release fertilizer. *Environ. Sci. Technol.* **2013**, *47*, 8700−8708.
(30) Sorgeloos, P.; Dhert, P.; Candreva, P. Use of the brine shrimp, Artemia spp., in marine fish larviculture. *Aquaculture* **2001**, *200*, 147−159.
(31) Migliore, L.; Civitareale, C.; Brambilla, G.; Di Delupis, G. D. Toxicity of several important agricultural antibiotics to Artemia. *Water Res.* **1997**, *31*, 1801−1806.
(32) Abatzopoulos, T. J.; Beardmore, J. A.; Clegg, J.; Sorgeloos, P. *Artemia: Basic and Applied Biology*; Springer Science & Business Media: Berlin, 2013; Vol. *1*.
(33) Brown, E. *World Fish Farming: Cultivation and Economics*; Springer Science & Business Media: Berlin, 2012; pp 25−32.
(34) Ben Naceur, H.; Ghazali, N.; Ben Rejeb Jenhani, A.; Romdhane, M. S. Study of the fatty acid composition of Artemia salina cysts from Tunisia. *J. Mar. Biol. Assoc. U. K.* **2013**, *93*, 1795−1803.
(35) Ringø, E.; Zhou, Z.; Olsen, R.; Song, S. Use of chitin and krill in aquaculture−the effect on gut microbiota and the immune system: a review. *Aquacult. Nutr.* **2012**, *18*, 117−131.
(36) Khan, M. N.; Islam, J. M.; Khan, M. A. Fabrication and characterization of gelatin-based biocompatible porous composite scaffold for bone tissue engineering. *J. Biomed. Mater. Res., Part A* **2012**, *100*, 3020−3028.
(37) Caruso, R.; Schattka, J. Cellulose acetate templates for porous inorganic network fabrication. *Adv. Mater.* **2000**, *12*, 1921−1923.
(38) Jiao, Y.; Whalen, J. K.; Hendershot, W. H. Phosphate sorption and release in a sandy-loam soil as influenced by fertilizer sources. *Soil Sci. Soc. Am. J.* **2007**, *71*, 118−124.
(39) Fayiga, A. O.; Ma, L. Q. Using phosphate rock to immobilize metals in soil and increase arsenic uptake by hyperaccumulator Pteris vittata. *Sci. Total Environ.* **2006**, *359*, 17−25.
(40) Sarkar, S.; Guibal, E.; Quignard, F.; SenGupta, A. Polymer-supported metals and metal oxide nanoparticles: synthesis, characterization, and applications. *J. Nanopart. Res.* **2012**, *14*, 1−24.
(41) Zhang, Q.; Du, Q.; Hua, M.; Jiao, T.; Gao, F.; Pan, B. Sorption enhancement of lead Ions from water by surface charged polystyrene-supported nano-zirconium oxide composites. *Environ. Sci. Technol.* **2013**, *47*, 6536−6544.
(42) Kosmulski, M. pH-dependent surface charging and points of zero charge: III. Update. *J. Colloid Interface Sci.* **2006**, *298*, 730−741.
(43) Kosmulski, M. The pH-dependent surface charging and points of zero charge: V. Update. *J. Colloid Interface Sci.* **2011**, *353*, 1−15.
(44) Yao, Y.; Gao, B.; Inyang, M.; Zimmerman, A. R.; Cao, X.; Pullammanappallil, P.; Yang, L. Biochar derived from anaerobically digested sugar beet tailings: characterization and phosphate removal potential. *Bioresour. Technol.* **2011**, *102*, 6273−6278.
(45) Kovar, J. L.; Pierzynski, G. M. Methods of phosphorus analysis for soils, sediments, residuals, and waters. *Southern Cooperative Series Bulletin*, 2nd edition; Virginia Tech University: Blacksburg, VA, **2009**.

DOI: 10.1021/acssuschemeng.5b00594
ACS Sustainable Chem. Eng. 2015, 3, 2496−2503